Inelastic collisions between selectively excited rubidium 6^2D-state atoms and noble-gas atoms: Fine-structure-state mixing

B. G. Zollars, H. A. Schuessler, J. W. Parker, and R. H. Hill, Jr.*
Department of Physics, Texas A&M University, College Station, Texas 77843
(Received 2 June 1982)

Inelastic collisional processes in fine-structure-state mixing have been studied by selective stepwise excitation and observation of the resulting fluorescence during collisions of excited rubidium $6^2D_{5/2}$ state atoms with various noble-gas atoms. It is shown that for intermediately excited rubidium atoms the fine-structure-state mixing cross sections are generally increasing from helium to xenon. The cross sections for the process $\mathrm{Rb}(6^2D_{5/2})+A(n\,^1S_0)\rightarrow\mathrm{Rb}(6^2D_{3/2})+A(n\,^1S_0)+\Delta E$ have the values $\sigma_{\mathrm{fs}}^{*}=2.4\pm0.9$, 3.1 ± 1.2, 2.6 ± 1.0, 5.8 ± 2.2, and 9.3 ± 5.6 in units of 10^{-14} cm^2, where A denotes in sequence any one of the noble gas atoms He, Ne, Ar, Kr, and Xe, respectively. Transfer cross sections for the transfer of excited Rb 6^2D-state atoms out of the doublet were also determined and are about an order of magnitude smaller than the fine-structure-mixing cross sections.

I. INTRODUCTION

Previously[1] we reported the observation of collisional fine-structure-state mixing for intermediately excited 6^2D state atoms of rubidium during collisions with $5^2S_{1/2}$ ground-state atoms of rubidium. The observed large cross section reflects the high polarizability of the paramagnetic rubidium ground state and is caused by both magnetic and electrostatic interactions. In the present experiment, the measurements were extended to include the diamagnetic noble gases as perturbers. In this case the interaction forces are dominantly electrostatic in nature and are both of the van der Waals and quadrupole-induced dipole type.

Since the pioneering work of R. W. Wood,[2] many experimental studies have been made of transitions in alkali-metal atoms induced by various perturbers. Before the advent of lasers, the measurements were confined to the lower states accessible by conventional means. For instance, the first ^2P states of rubidium ($n=5$) and cesium ($n=6$) have been extensively studied[3–5] with respect to fine-structure transitions induced by noble gases. More recently, when tunable dye lasers were introduced in the field, a multitude of intermediate and highly excited states became available for additional studies. The new techniques have stimulated further investigations of the various collisional processes and the complex mechanisms involved in them. Collisional processes of excited alkali-metal states and noble gases have recently been investigated in the rubidium n^2S states ($n=12$–18),[6] rubidium n^2P states ($n=12$–22),[7] rubidium n^2D states ($n=7$) (Ref. 8) and ($n=9$–13),[6] and rubidium n^2F states ($n=9$–21),[9] as well as in sodium n^2S states ($n=5$–20),[10] sodium n^2P states ($n=3$),[11–13] sodium n^2D states ($n=5$–15),[14] ($n=4$–34),[12,15] ($n=4$),[16] and sodium n^2F states ($n=13$–15).[17]

The theory of slow atomic collisions has been reviewed by Massey,[18] Nikitin,[19,20] and more recently by Delos.[21] Fermi[22] was the first to relate low-energy-electron scattering of the noble gases to collisions of excited-state alkali-metal atoms with noble gases. This concept is based on the excited alkali-metal valence electron being only weakly bound and has been used in analyzing fine-structure transitions in the first excited ^2P states of the alkali-metals[4] and also in the collisional angular momentum mixing of Rydberg D states of sodium.[14] In this model, the alkali-metal atom is treated as an ionic core with a quasifree valence electron associated with it. This quasifree valence electron scatters from the noble-gas atom. In the limit of zero electron energy, the cross sections or the related scattering lengths can be calculated.[23] It is found that in the first excited P states of the alkali-metals colliding with noble gases, the cross sections[4] correlate to the electron–rare-gas scattering cross sections, and that in the collisional angular momentum mixing, the cross sections correlate to the electron scattering lengths.

Quantum-mechanical close-coupling calculations[24,25] have been made for collisions involving the first excited ^2P state of the alkali-metal atoms and have shown that different mechanisms are important for the various noble gases as collision partners. For instance, Nikitin[26] has described the collision process with respect to the adiabatic alkali-metal-atom–noble-gas potential curves. Considering the relative motion of the alkali-metal and noble-gas

atom, the electrostatic (polarization or exchange) forces will at a certain distance create a competition with the magnetic spin-orbit coupling. When this process is described in terms of nonadiabatic mixing, it is called the first Nikitin mechanism. At shorter internuclear distances the magnetic spin-orbit interaction competes with the Coriolis interactions and in this regime the process is called the second Nikitin mechanism. As can be seen from these two types of mechanisms, both the energy separation between the two separated atomic states and the departure from adiabaticity are involved. For example, Nikitin's first mechanism is important in Rb(5^2P)-He collisions, whereas his second mechanism is more important in Rb(5^2P)-Ne or Ar collisions.[25] Since the departure from adiabaticity plays such an important role, it is not surprising that the cross sections are also weakly dependent on temperature.[5,27] Nikitin[28] has also proposed a third mechanism which comes into play when a highly excited alkali-metal P state collides with a noble-gas atom. In this mechanism, which for highly excited states is probably even more important than the first or second mechanism, the crossings of the excited $^2\Pi$ quasimolecular state by the repulsive $^2\Sigma$ states from below provide a large channel for nonelastic events. It is noted that these crossings actually become pseudocrossings when terms of the same symmetry participate. More involved semiclassical calculations[29] and recent measurements of excited P states[7] show that no simple model works well. An additional mechanism has been suggested for collisional depopulation of excited ^2S states which involves the short-range ionic-core noble-gas interaction.[10]

As experimental data on collisional angular momentum mixing of Rydberg states have become more plentiful,[14] more and more theoretical efforts have been put forward for highly excited atoms. Semiclassical calculations[30–32] and quantum-mechanical close-coupling theories[33–35] have been used to explain the experimental results. For fine-structure transitions in the excited D states of alkali-metal atoms in collisions with noble gases, including the heavy ones, theory and experiment still do not necessarily agree due to the difficulties in knowing the exact alkali-metal—noble-gas interaction potentials. However, work is progressing along these lines.[6,36]

With an increasing number of states available for study, various related collision cross sections have been investigated, including l-mixing collisions, quenching collisions, velocity changing collisions, as well as fine-structure collisions. It is the purpose of this work to investigate fine-structure collisions between the excited 6^2D states of rubidium induced in collisions with the various noble gases. The collision processes are studied in an intermediate binding energy region below the highly excited Rydberg levels, yet still above the tightly-bound low-lying first excited states.

II. EXPERIMENT

A short description of the experimental method to study inelastic collision processes between the fine-structure levels of the intermediate excited 6^2D states of rubidium with various noble gases follows. Details of the experimental apparatus are given in Ref. 1. Figure 1 shows the excitation scheme on a level diagram of rubidium. The 6^2D states of rubidium are populated by stepwise excitations using a rubidium radio-frequency electrodeless discharge lamp (0.3 mW/cm^2 at 7800 Å) and a tunable continuous-wave jet-stream dye laser (250 mW/cm^2 at 6300 Å). Two resonant photons of different frequencies are absorbed in sequence during the process. The first photon excites the atom to the $5^2P_{3/2}$ state from which, after absorption of a second photon, one of the 6^2D states is populated. Fine-structure collisions then transfer some of the rubidium atoms from the selectively excited state into the other fine-structure state of the doublet. The data are analyzed using rate equations to describe the various processes in order to deduce the fine-structure-collision cross sections.

Figure 2 depicts the experimental arrangement. A small glass cell with a diameter of 2.5 cm made of Corning 1720 or Pyrex glass is located at the center of the apparatus and contains a few milligrams of

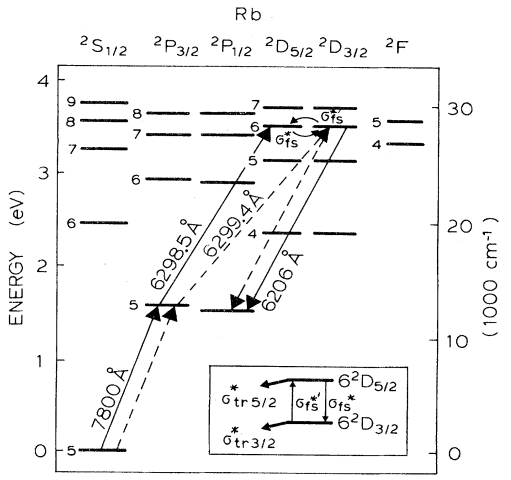

FIG. 1. A partial energy-level diagram showing the Rb states involved in the two-step excitation and fluorescent emission processes. The noble-gas-induced fine-structure mixing is described by the cross sections σ^*_{fs} and $\sigma^{*\prime}_{fs}$. Case 1 is illustrated by the solid lines and case 2 is depicted by the dashed lines.

rubidium metal. Before filling the cell with rubidium and sealing it off, the cell is first evacuated and baked for several days at about 500 °C until a vacuum of better than 10^{-6} Torr is reached. During the experiment the major part of the cell is heated in a glass oven to a slightly higher temperature than the small sidearm reservoir containing the rubidium. The temperature of the reservoir is monitored with a thermocouple and is kept constant at a temperature of typically 108 °C. The temperature of the resonance bulb is measured by a second thermocouple and the temperature gradient over the bulb region is minimized. A large number of cells have been made with fixed noble-gas pressures varying from cell to cell between 0 and 1 Torr.

The dye laser (Spectra-Physics model 375 without single mode etalon, pumped by an argon ion laser) and the rubidium lamp are arranged horizontally and at a 90° angle to each other. The linewidth of the laser is typically 20 GHz, which is much larger than the Doppler broadened linewidth, 0.5 GHz, of the 6^2D states. Therefore, the excitation can be considered to be "white" as far as each separately excited fine-structure level is concerned.

The fluorescent light is observed by a cooled photomultiplier (EMI 9658R, S-20) in the vertical direction through a monochromator (0.25-m Jarrell Ash) used as a narrow bandpass filter with a bandpass of about 8 Å. It is advantageous to use a modulation- and phase-sensitive detection scheme. When the rubidium lamp in the first excitation step is modulated with a light chopper, the fluorescence from the second excitation step is modulated, even though the laser light in the second step is not. With such a lock-in scheme it is possible to easily detect small fluorescence signals which would otherwise be hidden in the background of scattered laser light.

Data are accumulated in the following way.

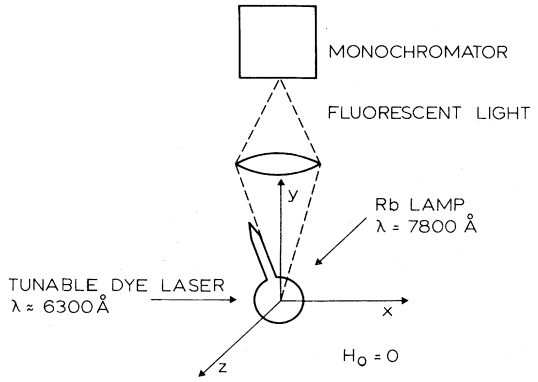

FIG. 2. Schematic diagram of the experimental arrangement.

When the dye laser is scanned, the fluorescent light intensity is recorded as a function of laser wavelength at a constant temperature and for various noble gases and noble-gas pressures. The fluorescent light intensity, the laser intensity, the rubidium lamp intensity, and the temperature of the rubidium reservoir of the sample cell are recorded simultaneously with a minicomputer, so that the signal can be normalized to constant excitation. The temperature of the observation region in the resonance cell is also measured.

The following inelastic collisions were investigated:

$$\mathrm{Rb}(6^2D_{5/2})+A(n\,{}^1S_0)\underset{\sigma^{*\prime}_{\mathrm{fs}}}{\overset{\sigma^{*}_{\mathrm{fs}}}{\rightleftarrows}}\mathrm{Rb}(6^2D_{3/2})+A(n\,{}^1S_0)+\Delta E\ , \quad (1)$$

where A denotes any of the noble gases He, Ne, Ar, Kr, and Xe, n is the main quantum number of the noble-gas ground state and the fine-structure splitting of the 6^2D state is labeled ΔE. In the collision process every rubidium atom in the $6^2D_{5/2}$ state can make a superelastic collision to the $6^2D_{3/2}$ state, whereas an atom in the $6^2D_{3/2}$ state has to overcome, in the reverse reaction, the threshold energy ΔE. The principle of detailed balancing

$$\sigma^{*}_{\mathrm{fs}}/\sigma^{*\prime}_{\mathrm{fs}}=\exp(\Delta E/kT)g(6^2D_{3/2})/g(6^2D_{5/2})\ , \quad (2)$$

relates the exothermic cross section σ^{*}_{fs} to the endothermic cross section $\sigma^{*\prime}_{\mathrm{fs}}$. The g's are statistical weights. The Boltzmann factor is $\exp(\Delta E/kT)\simeq 1$ in the present experiment. As in all cell-type experiments, Maxwellian averaged cross sections are measured by observing the fluorescent light intensity. In case 1 the laser is tuned to $\lambda=6298.5$ Å to excite the $6^2D_{5/2}$ state. In case 2 the laser is tuned to $\lambda=6299.4$ Å to excite the $6^2D_{3/2}$ state. The fluorescent light is detected in both cases at a third fixed wavelength of $\lambda=6206$ Å $(6^2D_{3/2}-5^2P_{1/2})$ selected by the monochromator. This arrangement has the advantage that the resolution is determined by the laser linewidth and not by the dispersion of the monochromator. The fine-structure splitting of $\Delta E=2.26\ \mathrm{cm}^{-1}$ in the 6^2D states is readily resolved. Due to the fine-structure collisions the fluorescence is observed from the $6^2D_{3/2}$ states even when only the $6^2D_{5/2}$ state is populated by the laser.

Typical registration curves are shown in Fig. 3 and are obtained in this example at three different helium-gas pressures. The signal on the left (towards the blue) corresponds to the $6^2D_{3/2}$ state being populated indirectly through fine-structure-changing collisions (case 1). The signal on the right

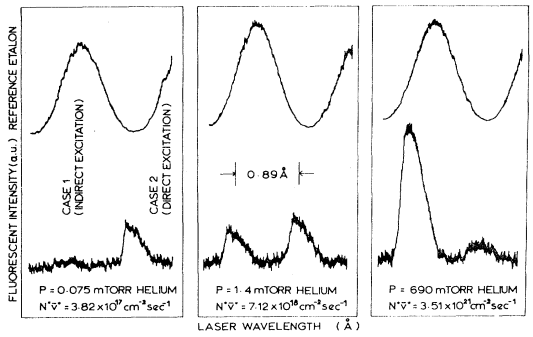

FIG. 3. Fluorescent light intensity from the $6^2D_{3/2}$ state to the $5^2P_{1/2}$ state at $\lambda = 6206$ Å as the laser is tuned from the $6^2D_{5/2}$ state (case 1) to the $6^2D_{3/2}$ state (case 2) for three different helium pressures. The transmission of the reference etalon is also depicted.

(towards the red) is obtained by direct laser excitation (case 2).

The intensities of the fluorescent light in case 1 and case 2 versus the krypton buffer gas pressure are shown in Fig. 4. The corresponding intensities were also observed for helium, neon, argon, and xenon as noble gases. A few mTorrs of noble gas have a sizable effect on the fluorescence intensities and therefore on the population numbers of the fine-structure states. The ratio of the case-1 fluorescence to the case-2 fluorescence from the $6^2D_{3/2}$ state increases with the noble-gas pressure because more rubidium $6^2D_{3/2}$ atoms are produced by fine-structure-changing collisions. The ratio of the fluorescent signals as a function of the noble-gas pressure yields the fine-structure-changing cross section. This ratio is shown for krypton as a noble gas in Fig. 5. The ratio approaches the value 9.00 at high pressures which is determined by the oscillator strength ratio

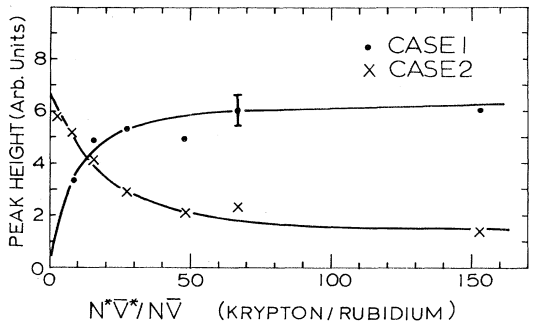

FIG. 4. Fluorescent light intensity from the $6^2D_{3/2}$ state to the $5^2P_{1/2}$ state at $\lambda = 6206$ Å versus krypton gas pressure for excitation case 1 and case 2. The smooth curve is for ease of viewing.

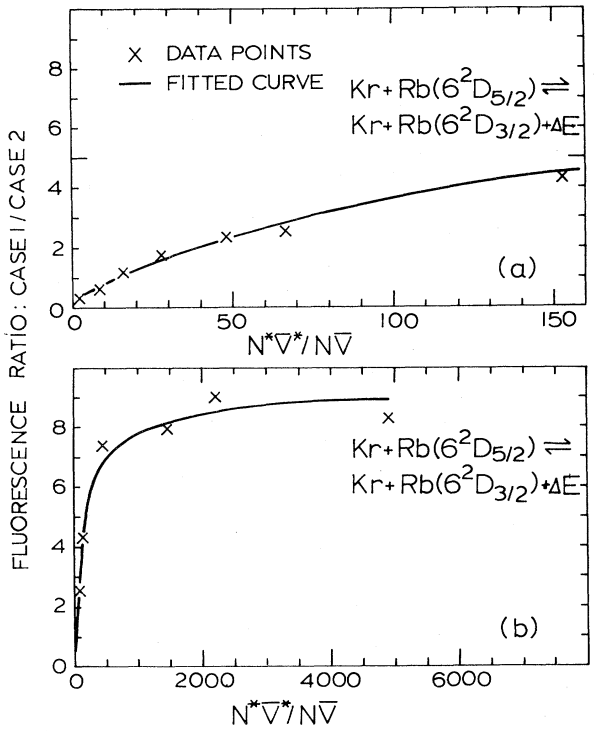

FIG. 5. Ratio of the fluorescent light intensities of excitation case 1 to case 2 versus krypton gas pressure. Part (a) depicts the low-pressure range only. Part (b) displays the data in the entire pressure range studied. The solid line represents the two-parameter fit and yields σ^*_{fs} and σ^*_{tr}.

$f_{P\rightarrow D_{5/2}}/f_{P\rightarrow D_{3/2}}$ of the transitions in the last step, as will be shown in Sec. III.

The contributions to the uncertainties are similar to those discussed in Ref. 1. The experimental scattering of the data points is only a minor source of error. The major contributions come from the density and temperature determinations. In the present experiment the noble-gas-atom density N^* and the average Rb—noble-gas relative velocity $\bar{v}^*$ are of interest. The noble-gas pressure p measured with a standard McLeod gauge was used to derive the noble-gas density according to $N^* = (L/760)p$, where L is Loschmidt's number. The noble-gas density determination is estimated to be accurate to $\pm 5\%$. The temperature of the resonance cell T could be measured to ± 2 °C yielding a 1% uncertainty for the noble-gas velocity $\bar{v}^*$. Both contributions combine to an uncertainty of $\pm 6\%$ in the value of $N^*\bar{v}^*$. The contribution to the fine-structure mixing by Rb-Rb* collisions was minimized by taking all data at the low rubidium density of about 1×10^{-4} Torr corresponding to a sidearm temperature of 108 °C.

III. DATA ANALYSIS

The collisional fine-structure cross sections are obtained by analyzing the measurements over the entire pressure range studied. For case 1, in steady state, the production rate of rubidium $6^2D_{3/2}$ atoms by fine-structure collisions of laser-excited rubidium $6^2D_{5/2}$ atoms with noble-gas atoms and ground-state atoms equals the loss rate which consists mainly of radiative decay, inverse fine-structure collisions, and transfer out of the $6^2D_{3/2}$ into various other states. The equations describing the collision processes were derived for steady-state conditions by setting the production rate (left side) and loss rate (right side) of the $6^2D_{3/2}$ state equal to each other; hence

case 1:

$$N^1_{5/2}N\bar{v}\sigma_{\rm fs}+N^1_{5/2}N^*\bar{v}^*\sigma^*_{\rm fs}=N^1_{3/2}(1/\tau_{3/2}+N\bar{v}\sigma'_{\rm fs}+N\bar{v}\sigma_{{\rm tr}(3/2)}+N^*\bar{v}^*\sigma^{*\prime}_{\rm fs}+N^*\bar{v}^*\sigma^*_{{\rm tr}(3/2)}) . \quad (3)$$

For case 2, in the steady state, the production rate of rubidium $6^2D_{3/2}$ atoms consists of the direct laser excitation and, to a lesser extent, of fine-structure collisions from the $6^2D_{5/2}$ states, that have been populated through inverse fine-structure collisions from the laser-populated $6^2D_{3/2}$ states. This latter population mechanism therefore involves two fine-structure collisions. The loss mechanism are similar to those in case 1, as above;

case 2:

$$W_{D_{3/2}}+N^2_{5/2}N\bar{v}\sigma_{\rm fs}+N^2_{5/2}N^*\bar{v}^*\sigma^*_{\rm fs}=N^2_{3/2}(1/\tau_{3/2}+N\bar{v}\sigma'_{\rm fs}+N\bar{v}\sigma_{{\rm tr}(3/2)}+N^*\bar{v}^*\sigma^{*\prime}_{\rm fs}+N^*\bar{v}^*\sigma^*_{{\rm tr}(3/2)}) . \quad (4)$$

In these equations the $N^{1,2}_{5/2,3/2}$ denote the number density in the $6^2D_{5/2}$ or $6^2D_{3/2}$ states and the superscript refers to case 1 or case 2. N is the number density of ground-state rubidium atoms and N^* is the number density of the noble-gas atoms. $\bar{v}$ stands for the root-mean-square relative velocity between ground-state rubidium atoms and excited rubidium atoms, $\bar{v}^*$ is the root-mean-square relative velocity between excited rubidium atoms and noble-gas atoms, and τ is the radiative lifetime of the 6^2D state. There exist two recent experimental measurements of this lifetime yielding (285±16) nsec (Ref. 37) and (237±15) nsec (Ref. 38) with no explanation for the discrepancy between the two measurements. We have also calculated the lifetime from transition probabilities by extending the approach of Heavens[39] to the 6^2D state and obtained $\tau=244$ nsec; since this value is in good agreement with one of the experimental values, $\tau=(237\pm15)$ nsec is used in the analysis. $\sigma_{\rm fs}$ is the Rb*-Rb fine-structure cross section ($6^2D_{5/2}\rightarrow 6^2D_{3/2}$) and $\sigma'_{\rm fs}$ is the fine-structure cross section for the reverse process ($6^2D_{3/2}\rightarrow 6^2D_{5/2}$). The corresponding fine-structure cross sections for the noble-gas atoms are labeled $\sigma^*_{\rm fs}$ and $\sigma^{*\prime}_{\rm fs}$, respectively. $W_{D3/2}$ is the excitation rate by direct laser excitations; $\sigma_{{\rm tr}(3/2)}$ is the transfer cross section out of the $6^2D_{3/2}$ state by any other collisional processes with ground-state rubidium atoms and $\sigma^*_{{\rm tr}(3/2)}$ is the corresponding cross section when a noble-gas atom is involved in the collision process.

The rate equation describing the collision processes in the $6^2D_{5/2}$ state are obtained similarly to the ones for the $6^2D_{3/2}$ state. In the steady state, the production rate (left side) and loss rate (right side) of the $6^2D_{5/2}$ state and are equal to each other; hence, for

case 1:

$$W_{D(5/2)}+N^1_{3/2}N\bar{v}\sigma'_{\rm fs}+N^1_{3/2}N^*\bar{v}^*\sigma^{*\prime}_{\rm fs}=N^1_{5/2}(1/\tau_{5/2}+N\bar{v}\sigma_{\rm fs}+N\bar{v}\sigma_{{\rm tr}(5/2)}+N^*\bar{v}^*\sigma^*_{\rm fs}+N^*\bar{v}^*\sigma^*_{{\rm tr}(5/2)}) , \quad (5)$$

where $W_{D_{5/2}}$ is the excitation by direct laser excitation of the $6^2D_{5/2}$ state.

For case 2 the $6^2D_{5/2}$ state is populated by fine-structure collisions from the laser excited $6^2D_{3/2}$ state yielding a fourth rate equation:

$$N^2_{3/2}N\bar{v}\sigma'_{\rm fs}+N^2_{3/2}N^*\bar{v}^*\sigma^{*\prime}_{\rm fs}=N^2_{5/2}\left[N\bar{v}\sigma_{\rm fs}+N^*\bar{v}^*\sigma^*_{\rm fs}+\frac{1}{\tau_{5/2}}+N\bar{v}\sigma_{\rm tr}+N^*\bar{v}^*\sigma^*_{{\rm tr}(5/2)}\right] . \quad (6)$$

Combining Eqs. (3)—(5) and assuming $\tau_{3/2}\approx\tau_{5/2}\approx\tau$, $\sigma_{{\rm tr}(3/2)}\approx\sigma_{{\rm tr}(5/2)}\approx\sigma_{\rm tr}$, and $\sigma^*_{{\rm tr}(3/2)}\approx\sigma^*_{{\rm tr}(5/2)}\approx\sigma^*_{\rm tr}$ yields

$$\frac{N^1_{3/2}}{N^2_{3/2}}=\left[\frac{W_{D_{5/2}}+N^1_{3/2}N\bar{v}\sigma'_{\rm fs}+N^1_{3/2}N^*\bar{v}^*\sigma^{*\prime}_{\rm fs}}{W_{D_{3/2}}+N^2_{5/2}N\bar{v}\sigma_{\rm fs}+N^2_{5/2}N^*\bar{v}^*\sigma^*_{\rm fs}}\right]\left[\frac{1+B_1}{1/\tau N\bar{v}\sigma_{\rm fs}+\sigma_{\rm tr}/\sigma_{\rm fs}+1+B_1+B_2}\right] , \quad (7)$$

where

$$B_1=\frac{N^*\bar{v}^*}{N\bar{v}}\frac{\sigma^*_{fs}}{\sigma_{fs}},$$

$$B_2=\frac{N^*\bar{v}^*}{N\bar{v}}\frac{\sigma^*_{tr}}{\sigma_{fs}}.$$

Solving Eq. (6) explicitly for $N^2_{5/2}$, and inserting it into Eq. (7) gives finally

$$\frac{N^1_{3/2}}{N^2_{3/2}}=\frac{W_{D_{5/2}}}{W_{D_{3/2}}}\left[\frac{1+B_1}{1/\tau N\bar{v}\sigma_{fs}+\sigma_{tr}/\sigma_{fs}+1+B_1+B_2}\right]. \tag{8}$$

When comparing Eq. (8) with Eq. (7) it is interesting to note that the first term in parentheses on the right-hand side of Eq. (7) reduces to the simple form of Eq. (8) containing only the ratio $W_{D_{5/2}}/W_{D_{3/2}}$. This shows that the small terms containing two fine-structure collisions cancel out, since both $N^1_{3/2}$ and $N^2_{5/2}$ are proportional to their respective production rates $W_{D_{5/2}}$ and $W_{D_{3/2}}$ by the same factor.

The ratio of the production rates is related to the ratio of the oscillator strengths by

$$W_{D_{5/2}}/W_{D_{3/2}}=f_{p\rightarrow D_{5/2}}/f_{p\rightarrow D_{3/2}}.$$

The oscillator strengths for these transitions have been calculated by various authors,[1,40] and even though the absolute values vary somewhat, the ratio is very consistent at

$$f_{p\rightarrow D_{5/2}}/f_{p\rightarrow D_{3/2}}=9.00$$

which was therefore used in the analysis.

The validity of Eq. (8) can be seen from the following considerations. In the high noble-gas pressure limit ($\approx$1 Torr), the ratio $N^1_{3/2}/N^2_{3/2}$ approaches the value of 9.00 to within the experimental scattering of the individual data points ($\approx$5%) for all noble gases investigated. Additionally, the ratio $N^1_{3/2}/N^2_{3/2}$ is consistent when data are taken at various laser intensities and rubidium ground-state densities.

A number of additional collision processes have been neglected in the analysis by the suitable choice of experimental conditions. In principle other generalized gain or loss terms could be taken into account by including gain terms on the left-hand side of Eqs. (3), (4), (5), and (6) or loss terms on the right-hand side of the same equations. Processes which have been neglected include the following: collisions with atoms in excited Rb P states which are important at high Rb densities due to radiation trapping; wall collisions which are important at low Rb densities N and noble-gas densities N^*; energy pooling back and forth between other nearby states due to angular momentum mixing (repopulation terms could be included as $\sigma^{*\prime}_{tr}$ and σ'_{tr} in the present notation); collisions with molecular Rb_2 and impurity gases which are present in the resonance cell; photoionization by a second laser photon in a three-step process, and subsequent collisions with photoelectrons; stimulated emission due to blackbody radiation[41]; three-body collision involving the excited ^2D-state atom and two other atoms; and associative ionization and subsequent recombination ($Rb^*+Rb\rightarrow Rb_2^+ + e^-$).

Care was taken to perform the measurements under conditions where all these effects are minimal and small against the measurement uncertainties. A low rubidium-atom density of about $N=4\times10^{12}$ cm^{-3} and a noble-gas density N^* in the range between 10^{14} and 10^{16} cm^{-3} were used. At the operating temperature (108 °C) of the resonance cell the molecular Rb_2 density is more than three orders of magnitude lower than the atomic density. Photoionization by the unfocused milliwatt continuous-wave laser is negligible and should be more significant in cases of pulsed laser excitation, where larger power levels have been used.[8] Blackbody effects give a contribution of less than 0.4% for the 6^2D state investigated. At a fixed temperature the contribution from Rb*-Rb collisions is constant and can be evaluated employing the Rb*-Rb fine-structure cross section

$$\sigma_{fs}=(0.74\pm0.25)\times10^{-13}\ \text{cm}^2$$

determined by us in a separate experiment using a resonance cell without noble gas, and σ_{tr} is of the same order of magnitude as σ_{fs}. A numerical minimalization scheme is used to fit the ratio of the fluorescence data to the two-parameter function of Eq. (8) and yields for each noble gas the cross sections σ^*_{fs} and σ^*_{tr} of interest.

IV. RESULTS AND DISCUSSION

The results of the present work are compiled in Table I. The error bars are quoted as 40% except for xenon where the error bars are 60%. It is noted that this uncertainty includes only the systematic effects in the determination of the noble-gas parameters N^* and $\bar{v}^*$ and the fitting uncertainties of the fluorescence ratio, but not the large error of approximately 30% of the fine-structure cross section σ_{fs} for Rb $6D$—Rb $5S$ collisions.

The values of σ^*_{fs} are roughly an order of magnitude smaller than the geometrical cross section σ_{geom} of the excited atom which is given by $\pi(r_e^2)$, where (r_e^2) is the hydrogenic expectation value of the square of the radius of the orbit. It holds[42] that

TABLE I. Fine-structure and transfer cross sections for the 6^2D state of Rb observed in collisions with noble gases (in units of 10^{-14} cm^2). The uncertainties of the cross sections are from the measurement of the noble-gas density, the temperature, and the fitting errors. The actual uncertainty is expected to be approximately $\approx 60\%$ due to the way $\sigma_{fs}(6^2D-5^2S)$ from Ref. 1 enters into Eq. (9).

Collision partners	σ^*_{fs} $(6^2D_{5/2}\rightarrow 6^2D_{3/2})$	$\sigma^{*\prime}_{fs}$ $(6^2D_{3/2}\rightarrow 6^2D_{5/2})$	σ^*_{tr} $(6^2D\rightarrow$ out of doublet)
Rb*-He	2.4±0.9	3.6±1.4[a]	0.00±0.12
Rb*-Ne	3.1±1.2	4.6±1.8	0.18±0.16
Rb*-Ar	2.6±1.0	4.0±1.7	0.19±0.13
Rb*-Kr	5.8±2.2	8.7±3.4	0.00±0.16
Rb*-Xe	9.3±5.6	14.1±8.4	0.90±1.18

[a]Calculated from σ^*_{fs} using the principle of detailed balancing.

$$\sigma_{geom}=\pi r_e^2=\tfrac{1}{2}\pi n^{*2}[5n^{*2}+1-3l(l+1)]a_0^2 \ . \quad (9)$$

Here n^* is the effective principal quantum number ($n^*=1\sqrt{\epsilon}$, where ϵ is the energy of the D state measured from the ionization limit in rydbergs), a_0 is the Bohr radius, and l is the orbital-angular momentum quantum number. The transfer cross sections σ^*_{tr} are even another order of magnitude smaller than σ^*_{fs}. This means that when an atom is excited into the $6^2D_{5/2}$ state and is colliding with a rare-gas atom, it is much more likely to make a fine-structure transition than it is to make a transition out of the doublet.

As has been pointed out, the cross sections are also weakly dependent on temperature, and as with all cell-type experiments, the results are an average over the Maxwellian velocity distribution at the temperature of interest. Therefore, when comparing with the results of others the temperature dependence, which is still not accurately known, must be kept in mind.

In Table II our results are compared to the values of Wolnikowski *et al.*[8] and Hugon *et al.*[6] for helium as the buffer gas as a function of the principal quantum number. For high values of n the cross section reduces to essentially the low-energy electron scattering cross section from the noble gas, and falls off as n increases, reflecting the fact that the volume occupied by the valence electron is very large; hence it is possible for the electron to "miss" the rare-gas atom. At the low value of $n=6$ this simple picture no longer holds, and it is hoped that our measurements will stimulate new theoretical work for the intermediately excited alkali-metal states.

Our experimental data is also compared in Table III to that of Wolnikowski *et al.*[8] and Biraben *et al.*[16] for several particular fine-structure states versus various noble gases. It can be seen that the cross sections do not simply follow polarizability or scattering-length trends.

The present experiment was performed in the absence of a magnetic field. It has been seen[43] that large magnetic fields influence the cross sections in the 6^2P state of cesium and this effect will be the subject of future investigations also for the intermediate ^2D states of rubidium investigated here. Polarization effects have also been observed[44] in fine-structure collisions induced by the light noble gases. However, in the present experiment the excitation linewidth is broad compared to the Doppler

TABLE II. Comparison of fine-structure and transfer cross sections for different n^2D states of Rb measured with helium as the noble gas (in units of 10^{-14} cm^2).

n	T (°C)	^2D splitting ΔE (cm^{-1})	Source	$\sigma^{*\prime}_{fs}$ $(6^2D_{3/2}\rightarrow 6^2D_{5/2})$	σ^*_{tr} $(n^2D\rightarrow$ out of doublet)	n^*	σ_{geom} (^2D)
6	108	2.26	This work	3.60±1.40	0.00±0.12	4.68	8.9
7	90	1.51	Wolnikowski *et al.*[a]	8.80±1.30	0.30±0.10	5.67	20.0
9	247	0.70	Hugon *et al.*[b]	5.10±1.00	0.11±0.02	7.66	71.0
10	247	0.48	Hugon *et al.*[b]	4.55±1.50	0.15±0.02	8.66	117.9
11	247	0.30	Hugon *et al.*[b]	2.20±0.60	0.29±0.05	9.66	184.4

[a]Reference 8.
[b]Reference 6.

TABLE III. Comparison of fine-structure cross section $\sigma^*_{fs}(n^2D_{5/2} \rightarrow n^2D_{3/2})$ for other alkali-metal ^2D states with the various noble gases (in units of 10^{-14} cm^2).

Alkali excited state	^2D splitting ΔE (cm^{-1})	T (°C)	He	Ne	Ar	Kr	Xe
Na(4D)[a]	0.035	270	5.1±1.2	5.7±1.1	7.8±1.1	11.8±1.1	18.7±3.4
Rb(6D)[b]	2.260	108	2.4±0.9	3.1±1.2	2.6±1.0	5.8±2.2	9.3±5.6
Rb(7D)[c]	1.510	90	5.8±0.9	4.0±0.6	6.9±1.0		

[a]Data from Biraben *et al.* (Ref. 16). Note Biraben reports the experimental value in the form of ${}^{3/2}_{5/2}\Sigma^\circ$ where

$$\sigma^*_{fs}({}^2D_{5/2} \rightarrow {}^2D_{3/2}) = \left[\frac{g(3/2)}{g(5/2)}\right] {}^{3/2}_{5/2}\Sigma^\circ = \left(\frac{4}{6}\right)^{1/2} {}^{3/2}_{5/2}\Sigma^\circ .$$

Therefore his experimental data has been multiplied by $(\frac{4}{6})^{1/2}$ before entering in the above table.

[b]Present work.

[c]Data from Wolnikowski *et al.* (Ref. 8).

broadened linewidths of the states of interest and there is no Zeeman splitting, so that any polarization effects are washed out and were not observed.

It is known that fine-structure transitions induced by diatomic molecules can have cross sections as much as an order of magnitude larger than the noble gases.[45] For this reason research-grade noble gases supplied by Matheson Gas Products in Pyrex glass cylinders were used and extreme care was taken with the Pyrex glass vacuum system used in filling the sample cells, so that only a negligible contribution is made from small contaminations due to residual gases.

In conclusion, the cross sections σ^*_{fs} $(6^2D_{5/2} \rightarrow 6^2D_{3/2})$ and $\sigma^*_{tr}(6^2D \rightarrow$ out of D) have been measured and have been compared to other related measurements. As detailed potential curves for the rubidium-atom—noble-gas interactions become available, and as present theories are extended to include the intermediately excited states, more detailed comparisons between experiment and theory will be made. These comparisons will be particularly interesting, when carried out for long ladders of excited states of different quantum numbers n and for a variety of perturbing gases as was done in the present investigation.

ACKNOWLEDGMENTS

This work is supported by the National Science Foundation under Grant No. PHY81-11943 and by the Center for Energy and Mineral Resources of Texas A&M University.

*Present address: Air Force Weapons Laboratory, Kirtland Air Force Base, Albuquerque, NM 87117.

[1]R. H. Hill, Jr., H. A. Schuessler, and B. G. Zollars, Phys. Rev. A 25, 834 (1982).

[2]R. W. Wood, Philos. Mag. 27, 1018 (1914); R. W. Wood and F. L. Mohler, Phys. Rev. 11, 70 (1918).

[3]T. J. Beahn, W. J. Condell, and H. I. Mandelberg, Phys. Rev. 141, 83 (1966).

[4]L. Krause, Appl. Opt. 5, 1375 (1966); L. Krause, in *The Excited State in Chemical Physics,* edited by J. W. McGowan (Wiley, New York, 1975).

[5]A. Gallagher, Phys. Rev. 157, 68 (1967); 172, 88 (1968).

[6]M. Hugon, F. Gounand, P. R. Fournier, and J. Berlande, J. Phys. B 13, 1585 (1980).

[7]F. Gounand, P. R. Fournier, and J. Berlande, Phys. Rev. A 15, 2212 (1977).

[8]J. Wolnikowski, J. B. Atkinson, J. Supronowicz, and L. Krause, Phys. Rev. A 25, 2622 (1982).

[9]M. Hugon, F. Gounand, P. R. Fournier, and J. Berlande, J. Phys. B 12, 2707 (1979).

[10]T. F. Gallagher and W. E. Cooke, Phys. Rev. A 19, 2161 (1979).

[11]J. Apt and D. Pritchard, Phys. Rev. Lett. 37, 91 (1976).

[12]A. Flusberg, R. Kachru, T. Mossberg, and S. R. Hartmann, Phys. Rev. A 19, 1607 (1979).

[13]T. W. Mossberg, E. Whittaker, R. Kachru, and S. R. Hartmann, Phys. Rev. A 22, 1962 (1980).

[14]T. F. Gallagher, S. A. Edelstein, and R. M. Hill, Phys. Rev. Lett. 35, 644 (1975); T. F. Gallagher, S. A. Edelstein, and R. M. Hill, Phys. Rev. A 15, 1945 (1977).

[15]P. F. Liao, J. E. Bjorkholm, and P. R. Berman, Phys. Rev. A 21, 1927 (1980).
[16]F. Biraben, K. Beroff, E. Giacobino, and G. Grynberg, J. Phys. (Paris) 39, L108 (1978); F. Biraben, K. Beroff, G. Grynberg, and E. Giacobino, *ibid.* 40, 519 (1979); G. Grynberg, E. Giacobino, F. Biraben, and K. Beroff, *ibid.* 40, 533 (1979).
[17]T. F. Gallagher, W. E. Cooke, and S. A. Edelstein, Phys. Rev. A 17, 904 (1978).
[18]H. S. W. Massey, E. H. S. Burhop, and H. B. Gilbody, in *Electronic and Ionic Impact Phenomena* (Clarendon, Oxford, 1971), Vol. III.
[19]E. E. Nikitin, in *Theory of Elementary Atomic and Molecular Processes in Gases* (Clarendon, London, 1974).
[20]E. E. Nikitin, Adv. Chem. Phys. 28, 317 (1975).
[21]J. B. Delos, Rev. Mod. Phys. 53, 287 (1981).
[22]E. Fermi, Nuovo Cimento 11, 157 (1934).
[23]T. F. O'Malley, Phys. Rev. 130, 1020 (1963).
[24]J. Pascale and R. E. Olson, J. Chem. Phys. 64, 3538 (1976).
[25]A. D. Wilson, and Y. Shimoni, J. Phys. B 7, 1543 (1974).
[26]E. E. Nikitin, in *Theory of Elementary Atomic and Molecular Processes in Gases,* Ref. 19, p. 141, and originally in E. E. Nikitin, J. Chem. Phys. 43, 744 (1965).
[27]E. E. Nikitin, in *Theory of Elementary Atomic and Molecular Processes in Gases,* Ref. 19, p. 146.
[28]E. E. Nikitin and A. I. Reznikov, Chem. Phys. Lett. 8, 161 (1971).
[29]J. Pascale and P. M. Stone, J. Chem. Phys. 65, 5122 (1976).
[30]J. I. Gersten, Phys. Rev. A 14, 1354 (1976).
[31]A. Omont, J. Phys. (Paris) 38, 1343 (1977).
[32]E. de Prunele and J. Pascale, J. Phys. B 12, 2511 (1979).
[33]M. Matsuzawa, J. Phys. B 12, 3743 (1979).
[34]A. P. Hickman, Phys. Rev. A 18, 1339 (1978); 19, 994 (1979).
[35]R. E. Olson, Phys. Rev. A 15, 631 (1977).
[36]J. Pascale and J. Vandeplanque, J. Chem. Phys. 60, 2278 (1974); J. Pascale, *ibid.* 69, 2788 (1978).
[37]H. Lundberg and S. Svanberg, Phys. Lett. 56A, 31 (1976).
[38]J. Marek, and P. Münster, J. Phys. B 13, 1731 (1980).
[39]O. S. Heavens, J. Opt. Soc. Am. 51, 1058 (1961).
[40]R. H. Hill, Jr., Ph.D. dissertation, Texas A&M University, 1979 (unpublished); J. Migdalek and W. E. Baylis, Can. J. Phys. 57, 1708 (1979); Brian Warner, Mon. Not. R. Astron. Soc. 139, 115 (1968).
[41]W. E. Cooke and T. F. Gallagher, Phys. Rev. A 21, 588 (1980).
[42]H. A. Bethe and E. E. Salpeter, in *Quantum Mechanics of One and Two Electron Atoms* (Plenum, New York, 1977).
[43]J. Guiry and L. Krause, Phys. Rev. A 12, 2407 (1975).
[44]F. Biraben, K. Beroff, E. Giacobino, and G. Grynberg, J. Phys. (Paris) 39, L110 (1978).
[45]A. P. Hickman, Phys. Rev. Lett. 47, 1585 (1981).